1999

Late-Time Optical and Ultraviolet Spectra of SN 1979C and SN 1980K

Robert A. Fesen
Dartmouth College

Christopher L. Gerardy
Dartmouth College

Alexei V. Filippenko
University of California at Berkeley

Thomas Matheson
University of California at Berkeley

Roger A. Chevalier
University of Virginia

See next page for additional authors

THE ASTRONOMICAL JOURNAL, 117:725–735, 1999 February

LATE-TIME OPTICAL AND ULTRAVIOLET SPECTRA OF SN 1979C AND SN 1980K

ROBERT A. FESEN,[1] CHRISTOPHER L. GERARDY,[1] ALEXEI V. FILIPPENKO,[2] THOMAS MATHESON,[2]
ROGER A. CHEVALIER,[3] ROBERT P. KIRSHNER,[4] BRIAN P. SCHMIDT,[5] PETER CHALLIS,[4]
CLAES FRANSSON,[6] BRUNO LEIBUNDGUT,[7] AND SCHUYLER D. VAN DYK[8]
Received 1998 October 21; accepted 1998 October 28

ABSTRACT

A low-dispersion Keck I spectrum of SN 1980K taken in 1995 August ($t = 14.8$ yr after explosion) and a spectrum taken in 1997 November ($t = 17.0$ yr) at the MDM Observatory show broad 5500 km s^{-1} emission lines of Hα, [O I] 6300, 6364 Å, and [O II] 7319, 7330 Å. Weaker but similarly broad lines detected include [Fe II] 7155 Å, [S II] 4068, 4072 Å, and a blend of [Fe II] lines at 5050–5400 Å. The presence of strong [S II] 4068, 4072 Å emission but a lack of [S II] 6716, 6731 Å emission suggests electron densities of 10^5–10^6 cm^{-3}. From the 1997 spectrum, we estimate an Hα flux of $(1.3 \pm 0.2) \times 10^{-15}$ ergs cm^{-2} s^{-1}, indicating a 25% decline from the 1987–1992 levels during the period 1994 to 1997, possibly related to a reported decrease in its nonthermal radio emission. A 1993 May, Multiple Mirror Telescope spectrum of SN 1979C ($t = 14.0$ yr) shows a somewhat different spectrum from that of SN 1980K. Broad, 6000 km s^{-1} emission lines are also seen but with weaker Hα, stronger [O III] 4959, 5007 Å, more highly clumped [O I] and [O II] line profiles, no detectable [Fe II] 7155 Å emission, and a faint but very broad emission feature near 5750 Å. A 1997 *Hubble Space Telescope* Faint Object Spectrograph, near-UV spectrum (2200–4500 Å) shows strong lines of C II] 2324, 2325 Å, [O II] 2470 Å, and Mg II 2796, 2803 Å, along with weak [Ne III] 3969 Å, [S II] 4068, 4072 Å, and [O III] 4363 Å emissions. The UV emission lines show a double-peak profile with the blueward peak substantially stronger than the red, suggesting dust extinction within the expanding ejecta [$E(B-V) = 0.11$–0.16 mag]. The lack of detectable [O II] 3726, 3729 Å emission, together with [O III] $\lambda\lambda(4959 + 5007)/\lambda 4363 \simeq 4$, implies electron densities 10^6–10^7 cm^{-3}. These Type II linear supernovae (SNe II-L) spectra show general agreement with the lines expected in a circumstellar interaction model, but the specific models that are available show several differences with the observations. High electron densities (10^5–10^7 cm^{-3}) result in stronger collisional de-excitation than assumed in the models, thereby explaining the absence of several moderate to strong predicted lines such as [O II] 3726, 3729 Å, [N II] 6548, 6583 Å, and [S II] 6716, 6731 Å. Interaction models are needed that are specifically suited to these supernovae. We review the overall observed range of late-time SNe II-L properties and briefly discuss their properties relative to young, ejecta-dominated Galactic supernova remnants.

Key words: galaxies: individual (NGC 4321, NGC 6946) — supernovae: individual (SN 1979C, SN 1980K)

1. INTRODUCTION

The Type II linear supernova (SN II-L) SN 1980K in NGC 6946 reached a peak brightness of $V = 11.4$ in 1980 November (see Barbon, Ciatti, & Rosino 1982; Hurst & Taylor 1986 and references therein). Despite a steadily declining flux through 1982 (Uomoto & Kirshner 1986), faint Hα emission from SN 1980K was detected in 1987 through narrow passband imaging (Fesen & Becker 1990, hereafter FB90). Low-dispersion optical spectra obtained in 1988 and 1989 showed broad, 6000 km s^{-1} Hα and [O I] 6300, 6364 Å emission, along with weaker line emission from [Ca II] 7291, 7324 Å and/or [O II] 7319, 7330 Å, [O III] 4959, 5007 Å, and [Fe II] 7155 Å (FB90; Uomoto 1991; Leibundgut et al. 1991). Monitoring of its optical flux from 1988 through 1992 indicated a nearly constant luminosity (Leibundgut, Kirshner, & Porter 1993; Fesen & Matonick 1994, hereafter FM94).

Following the optical recovery of SN 1980K, a handful of other SNe II-L have been optically detected 7–25 yr after maximum light. These include SN 1986E in NGC 4302 (Cappellaro et al. 1995), SN 1979C in M100 (Fesen & Matonick 1993), and SN 1970G in M101 (Fesen 1993). The late-time optical spectra of all these SNe show broad Hα and forbidden oxygen emission lines, and these characteristics have been exploited in searching for fainter, late-time SNe II-L (e.g., SN 1985L in NGC 5033; Fesen 1998).

Of the few SNe II-L recovered at late times, SN 1979C in M100 (NGC 4321) is particularly noteworthy. This SN was exceptionally bright at outburst for a Type II event, with a peak M_B of -20 mag (Young & Branch 1989; Gaskell 1992) and became bright in the radio as well, eventually reaching a 6 cm luminosity more than 200 times that of Cas A (Weiler et al. 1989). It also exhibits among the highest, late-time Hα luminosity ($\sim 1 \times 10^{38}$ ergs s^{-1}) and shows radio emission variability, which may be due to a periodic

[1] Department of Physics and Astronomy, Dartmouth College, 6127 Wilder Laboratory, Hanover, NH 03755.
[2] Department of Astronomy, University of California at Berkeley, Department of Astronomy, 601 Cambell Hall, Berkeley, CA 94720-3411.
[3] Department of Astronomy, University of Virginia, P.O. Box 3818, Charlottesville, VA 22903.
[4] Harvard-Smithsonian Center for Astrophysics, 60 Garden Street, Cambridge, MA 02138.
[5] Mount Stromlo and Siding Spring Observatories, Australian National University, Private Bag, Weston Creek, ACT 2611, Australia.
[6] Stockholm Observatory, SE 133 36 Saltsjöbaden, Sweden.
[7] European Southern Observatory, Karl-Schwarzschild-Strasse 2, Garching, 85748, Germany.
[8] Infrared Processing and Analysis Center, California Institute of Technology, Mail Stop 100-22, Pasadena, CA 91125.

modulation of the progenitor's pre-SN mass loss (Weiler et al. 1991).

Late-time optical SN II emission lines are thought to arise from interactions with surrounding circumstellar mass-loss material (CSM). These interactions lead to the formation of a reverse shock moving back into the expanding ejecta, which then subsequently ionizes, either by far-UV or X-ray emission, a broad inner ejecta region from which the optical lines are produced (Chevalier & Fransson 1994, hereafter CF94). This model is also consistent with the presence of accompanying nonthermal radio emission in all optically recovered SNe II-L, with radio light curves like those predicted from the "minishell" model involving shock generated synchrotron emission from the forward shock (Chevalier 1982; Weiler et al. 1993).

Late-time SN II emission lines are important for the information they can provide on SNe ejecta abundances, late-time shock emission processes, and the mass-loss history and evolutionary status of SN progenitors (Leibundgut et al. 1991; Weiler et al. 1991; Montes et al. 1998). Unfortunately, optical emission lines from old SNe II-L are quite faint ($\leq 3 \times 10^{-17}$ ergs cm^{-2} s^{-1} Å^{-1}), making accurate measurements difficult even using 4 m class telescopes. Consequently, much is still uncertain about their spectra, even for SN 1980K, the best and longest studied object. For example, virtually nothing is known about SN II-L spectra below 5000 Å, and uncertainties remain as to whether [Ca II] or [O II] is chiefly responsible for the strong emission commonly seen near 7300 Å. SN 1980K's current optical properties are of special interest due to a recently reported sharp decline in nonthermal radio flux in the interval 1994–1997 (Montes et al. 1998).

Here we present a 1995 Keck spectrum of SN 1980K, which shows the region below 5000 Å for the first time, and a spectrum, taken in November 1997 at the MDM Observatory, useful for investigating its recent Hα flux. We then compare these SN 1980K data with a 1993 MMT spectrum of SN 1979C at a similar age to the Keck SN 1980K spectrum. We also present a 1997 *Hubble Space Telescope* (*HST*) UV spectrum of SN 1979C, which reveals several strong UV and near-UV lines, which help clarify the nature of the observed emission. Finally, we outline some general observed properties of late-time SNe II-L and compare them with young Galactic supernova remnants (SNRs).

2. OBSERVATIONS

Two consecutive low-dispersion spectra of SN 1980K were obtained on 1995 November 28 with the Low Resolution Imaging Spectrometer (LRIS; Oke et al. 1995) at the Cassegrain focus of the Keck I telescope. The duration of each exposure was 30 minutes. Conditions were not photometric, and the seeing was about 1″. The position angle of the slit (of width 1″) was 128°.5, through two stars that are known to be colinear with the supernova position; this was also close to the parallactic angle at the time of observation. We used a Tektronix 2048 × 2048 pixel CCD with a scale of 0″.41 per binned pixel in the spatial direction, a gain of 1.1 e^- count^{-1}, and a readout noise of 6 e^- pixel^{-1}.

Cosmic rays were eliminated from the two-dimensional spectra through a comparison of the pair of exposures. The background sky was measured in regions adjacent to the supernova and subtracted from the extracted spectrum. Spectra of HgKrNeAr comparison lamps were used to determine the wavelength scale and resolution (~10 Å). Flux calibration and removal of telluric absorption lines were achieved with a spectrum of the sdF star BD +17°4708 (Oke & Gunn 1983).

A spectrum of SN 1980K was also obtained on 1997 November 3 using the 2.4 m Hiltner telescope at the MDM Observatory on Kitt Peak. A modular spectrograph like that in use at Las Campanas Observatory was employed with a north-south aligned 2″.2 × 4′ slit, a 600 line mm^{-1} 5000 Å blaze grating, and a 1024 × 1024 Tektronics CCD detector. A single 6000 s exposure covering the spectral region 4000–8500 Å was taken with a spectral resolution of about 5 Å. Cosmic rays were removed using standard IRAF routines for pixel rejection and replacement. Observing conditions were photometric but due to slit light losses caused by variable seeing during the long exposure, absolute fluxes are reliable only to ±15%.

A spectrum of SN 1979C was obtained on 1993 May 21 using the Red Channel long-slit CCD spectrograph (Schmidt, Weymann, & Foltz 1989) on the 4.5 m Multiple Mirror Telescope (MMT). Three 1200 s exposures were taken using a 2″ × 180″ slit and covering a spectral range 3800–9900 Å with 12 Å resolution. A strong blue continuum, possibly from O and B stars near SN 1979C's location in NGC 4321 (M100), was removed in the final reduction, and an arbitrary zero flux level set. Because of the greatly increased noise level redward of 8000 Å, we show here only the region 4000 to 8000 Å.

An *HST* spectrum of SN 1979C was obtained using the Faint Object Spectrograph (FOS) on 1997 January 30. Three G270H exposures (2200–3275 Å) were taken for a total time of 7170 s, plus one G400H spectrum (3250–4750 Å) with an exposure of 2410 s. Both the G270H and G400H data shown here have been smoothed by a five-point average.

3. RESULTS

3.1. *SN 1980K*

The Keck and MDM spectra of SN 1980K are shown in Figures 1 and 2, respectively. Though the Keck spectrum has a significantly higher signal-to-noise ratio (S/N), both show broad Hα and [O I] 6300, 6364 Å lines plus emission near 7100 and 7300 Å. These features have been seen in

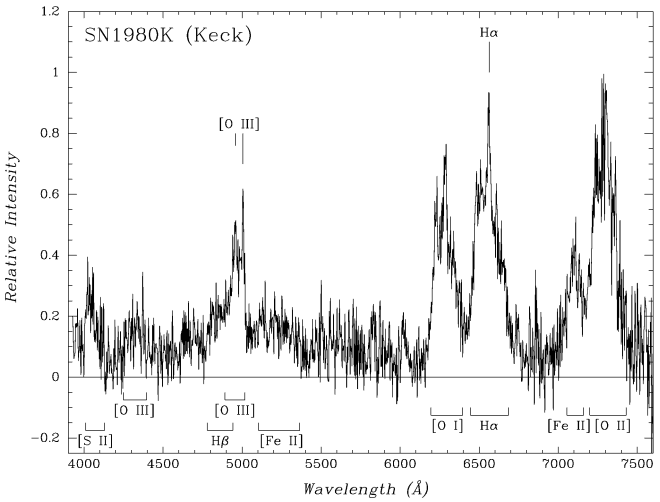

FIG. 1.—Keck spectrum of SN 1980K taken in 1995 August

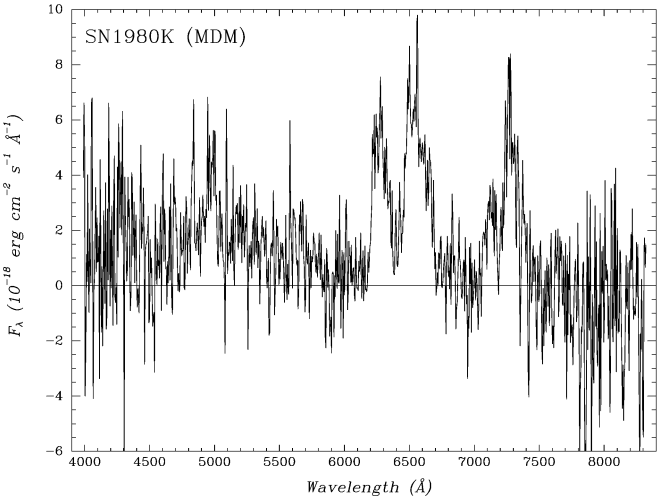

FIG. 2.—MDM spectrum of SN 1980K taken in 1997 November

earlier SN 1980K spectra with roughly the same relative strengths and widths as seen here. However, the line profiles are better defined in the Keck data, and the spectrum reveals other fainter emission lines not previously seen.

Hα.—SN 1980K's late-time optical flux was first detected in 1987 via its strong Hα emission, and it remains among the strongest optical lines observed a decade later. The 1995 Keck spectrum shows the Hα line profile with an expansion velocity of -5700 to $+5500$ km s^{-1} with a strong asymmetry toward the blue, in good agreement with earlier 1992 and 1994 measurements (FM94; Fesen, Hurford, & Matonick 1995, hereafter FHM94). A comparison of SN 1980K's Hα line profile and strength changes over the last 10 yr is shown in Figure 3 using the Lick 1988 June spectrum (FB90) and our 1997 November MDM data. Besides illustrating a drop in Hα flux over this time period (see § 4 below), one also sees a substantial decrease in the line width, most noticeable toward the blue edge. In 1988, the FWHM of Hα was around 220 Å, compared with 190 Å in 1997. This decrease is consistent with earlier measurements (FM94) and is predicted by SN-CSM interaction models (CF94). However, the asymmetric profile of Hα appears not to have changed much during the last 10 yr, with a sharp blue emission edge and an emission peak near 6500 Å visible in both the 1988 and 1997 line profiles.

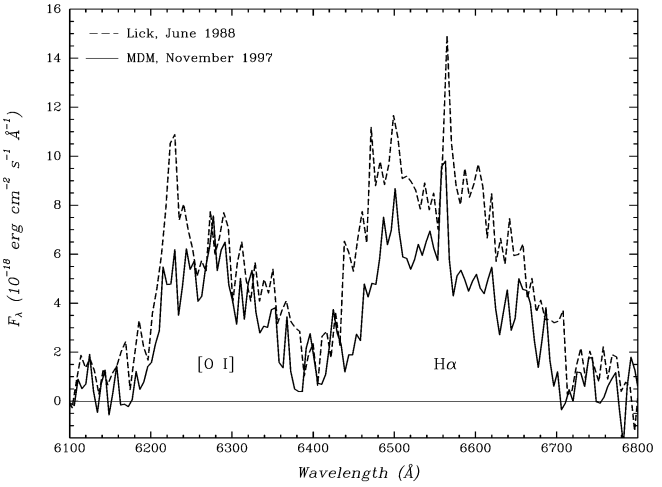

FIG. 3.—Comparison of 1988 June and 1997 November SN 1980K spectra for the [O I] 6300, 6364 Å and Hα emission profiles.

A faint, unresolved line is seen on top of the broader Hα emission around zero radial velocity. A narrow Hα emission feature was evident in the 1988 Lick spectrum, but much less so in subsequent data (FM94; FHM95). Well detected again here, this narrow Hα emission may be due to a small H II region near the SN site or ionized wind material associated with the progenitor (FB90; FHM95).

From the 1997 MDM spectrum, we estimate a broad emission Hα flux of $1.3 \pm 0.2 \times 10^{-15}$ ergs cm^{-2} s^{-1}. This is close to the 1.4×10^{-15} ergs cm^{-2} s^{-1} value reported by FHM95 for a 1994 spectrum and supports the conclusion of a $\simeq 25\%$ fading from flux levels observed in the late 1980s and early 1990s.

Hβ.—There is broad emission near 4850 Å, some of which may be due to Hβ 4861 Å. Its line strength, however, is difficult to disentangle from other possible emission lines between 4800 and 5000 Å (see below). Nonetheless, the observed Hα/Hβ line ratio must be ≥ 6, suggesting, after correcting for a foreground reddening of $E(B-V) = 0.40$ mag (Burstein & Heiles 1982), an intrinsic value ≥ 4.

Hγ.—Weak emission near 4350 Å may be attributable in part to Hγ emission, blended with [O III] 4363 Å.

[O I].—The broad [O I] 6300, 6364 Å emission is asymmetric toward the blue with a steep blue edge and a more gradual decline toward the red. The line's full velocity range is -6000 km s^{-1} if attributed to 6300 Å on the blue side and $\geq +1700$ km s^{-1} if attributed to 6363 Å on the red. The blueward velocity is larger than the -4800 km s^{-1} estimated by FM94, probably due in part to weaker emission detected due to the higher S/N in the Keck spectrum. In addition, a prominent emission peak at 6280 Å suggests strong clumping of the O-emitting material in the SN's facing expanding hemisphere.

[O II].—One of the strongest emission features in the spectrum, rivaling Hα and [O I], lies near 7300 Å, and extends from 7180 to 7420 Å. It has been alternatively identified as [Ca II] 7291, 7324 Å (Uomoto 1991; FHM95), [O II] 7319, 7330 Å (in SN 1979C; FM93), or a combination of the two (FB90; FM94). CF94 suggest it is likely to be solely [Ca II] since these [O II] lines are weak in a variety of SN-CSM models and in a variety of photoionized objects. However, these models also predict appreciable Ca II infrared triplet emission (8498, 8542, 8662 Å), which is absent in SN 1980K's near-IR spectrum (FM94; FHM95).

Figure 4a shows SN 1980K's [O I] 6300, 6364 Å line profile in terms of expansion velocity relative to 6300 Å compared with the 7300 Å feature if identified as the [O II] line blend at 7325 Å (*top*), or [Ca II] using the stronger 7291 Å [Ca II] line (*bottom*). The [O II] blend interpretation is seen to provide a better match to [O I] 's line width and its emission substructure than does a [Ca II] interpretation. For instance, the 6280 Å emission peak in the [O I] line profile matches well with the 7300 Å feature's emission feature at 7300 Å if interpreted as an [O II] blend. In addition, the velocity of the 7300 Å feature's FWHM blueward edge agrees within measurement uncertainties to those of [O I] and Hα using the 7319 Å [O II] line: namely, 4750, 4500, and 4600 km s^{-1} for [O I], Hα, and 7300 Å, respectively, compared with 3450 km s^{-1} using [Ca II] 7291 Å.

A possible complication is an atmospheric absorption band at 7190 Å, which might have affected the 7300 Å feature's blue emission. This telluric absorption band is not

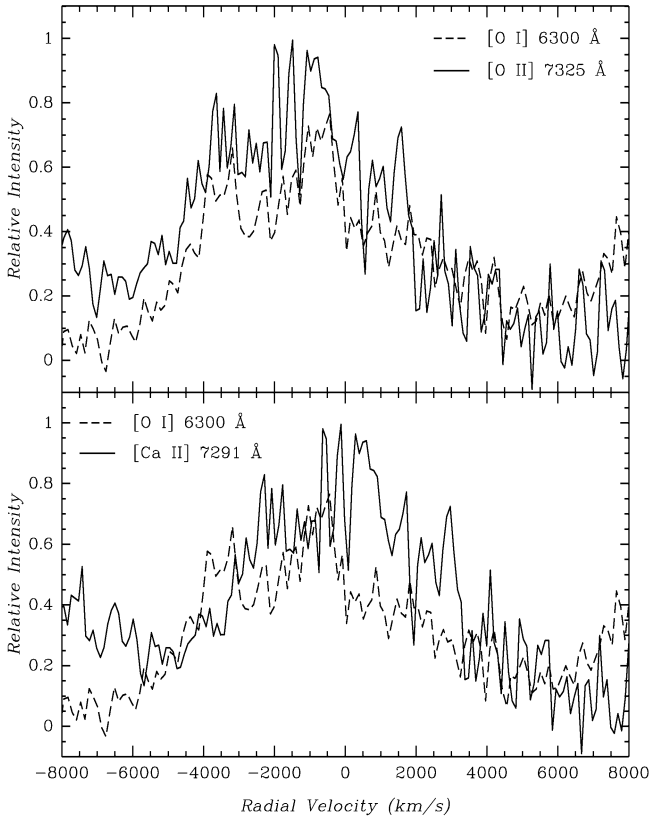

FIG. 4*a*

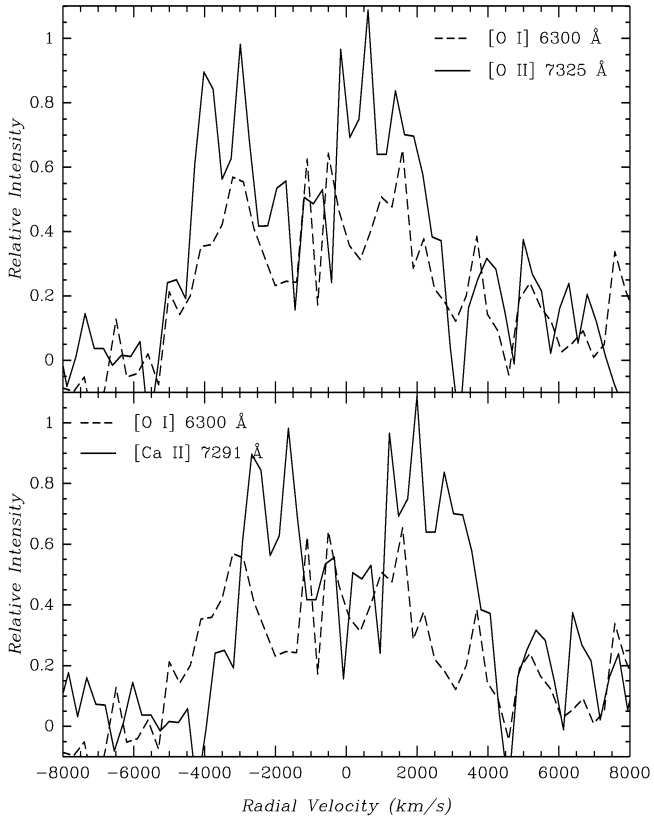

FIG. 4*b*

FIG. 4.—Line profile comparison of (*a*) SN 1980K's and (*b*) SN 1979C's [O I] 6300, 6364 Å emission feature vs. the 7300 Å emission feature in velocity space when interpreted as due to [O II] 7319, 7330 Å (*top*) or [Ca II] 7291, 7324 Å (*bottom*). Velocity scales given are calculated for the [O I] 6300 Å line, the [Ca II] 7291 Å line, or the [O II] line blend at 7325 Å.

especially strong, however, and though it could help to explain the poor [Ca II] profile match to that of [O I] at large negative velocities (see Fig. 4), there still would remain the discrepancy along the line's red end. We therefore conclude that [O II] 7319, 7330 Å emission is the dominant cause for the 7300 Å emission feature.

[O III].—Previous SN 1980K spectra detected broad emission near 5000 Å with an emission peak near 4955 Å. The broad emission was initially identified as [O III] 4959, 5007 Å emission (FB90; Leibundgut et al. 1991; FM94), although Uomoto (1991) suggested that it might be a blend of permitted Fe II lines. As seen in Figure 1, broad emission extends from 4750 to 5020 and from 5100 to 5400 Å, with little emission between 5020 and 5100 Å. Absence of strong emission just redward of 5007 Å is hard to reconcile with a broad, 5000 km s^{-1} [O III] line profile like that seen for [O I], [O II], and Hα unless the [O III] emission is weak and has a strong blue asymmetry. In fact, the sharp cutoff of emission at 5020 Å places an expansion limit on strong [O III] 5007 Å emission of $\leq +1000$ km s^{-1}. Nonetheless, [O III] appears a much more likely identification than either permitted or forbidden Fe II and Fe III lines (cf. FHM95), especially in view of the clear [O III] emission in other SNe II-L (e.g., SN 1979C; see § 3.2). The far blue side of the feature is probably due to Hβ 4861 Å. Finally, weak emission near 4350 Å may be a blend of [O III] 4363 Å and Hγ.

The Keck spectrum also shows two narrow lines at 4957 and 5005 Å. These are probably related to the narrow Hα emission observed. However, in many earlier spectra, only one emission spike, around 4950–4960 Å, could be clearly seen (FB90; Leibundgut et al. 1991; FM94) and was interpreted as possible evidence of emission substructure in the 4959, 5007 [O III] blend. An alternative explanation is that the narrow 4959 Å line emission happens to coincide with a -3600 km s^{-1} emission feature in the broad [O III] line, like that seen in the [O I] and [O II] line profiles.

[Fe II].—Emission near 7100 Å that merges into the red wing of the 7300 Å line is likely [Fe II] 7155 Å (FB90; FM94). Adopting a line center of 7100 Å gives an emission centroid velocity of -2300 km s^{-1}. Emission extends toward the blue as far as $\simeq$7010 Å, suggesting a maximum velocity of -6000 km s^{-1}. Due to the blend with the [O II] 7300 Å feature, little can be determined regarding its maximum recession velocity. However, the line extends at least to 7175 Å ($+800$ km s^{-1}).

Broad weak emission from 5020 to 5400 Å can be understood in terms of blends of several [Fe II] lines—specifically, the 5112 (19F), 5158 (18F), 5159 (19F), 5262 (19F), 5269 (18F), 5273 (18F), and 5334 (19F) Å lines. These represent all of the stronger [Fe II] lines from the multiplets 18F and 19F typically seen in shocked supernova remnant emissions (cf. Fesen & Hurford 1996). Adopting a line center shift of -2300 km s^{-1} and a velocity width of -6000 to $+3500$ km s^{-1} like that seen for the [Fe II] 7155 Å line, a blend of [Fe II] lines can explain the 5020–5400 Å emission: specifically, its width, peak intensity near the strong 5158 and 5159 [Fe II] lines, and the lack of emission longward of 5400 Å and shortward of 5050 Å.

[S II].—The weak emission feature near the blue end of the Keck spectrum appears to be [S II] 4069, 4076 Å.

Adopting this identification, sulfur has a velocity range of -5500 to $+4000$ km s^{-1}, comparable to the broad H and O lines. As with other lines, the [S II] profile also shows a strong blue asymmetry, with a line center shifted to the blue at least -2000 km s^{-1}. Finally, we note there is no obvious emission from the nebular [S II] 6716, 6731 Å lines in either the Keck or MDM spectra, and previous SN 1980K studies have failed to detect any [S III] 9069, 9531 Å emission (FHM95).

3.2. *SN 1979C*

3.2.1. *Optical Spectrum*

A 1993 MMT spectrum of SN 1979C taken 14 yr after maximum light, or roughly the same age as SN 1980K when the 1995 Keck spectrum was obtained, is shown in Figure 5. The spectrum is similar to those presented by FM93 but with much improved S/N especially in the blue.

Hα.—Broad Hα emission is detected with an expansion velocity of ± 6200 km s^{-1}. A strong, narrow Hα component is also seen at $+120$ velocity in M100's rest frame ($V = +1570$ km s^{-1}). The broad Hα emission has a flux of $3 \pm 0.5 \times 10^{-15}$ ergs cm^{-2} s^{-1}, or slightly larger than the 2.5×10^{-15} ergs cm^{-2} s^{-1} reported by FM93. Hα's peak flux is somewhat weaker than [O I] 6300 Å, and the profile shows a strong blue asymmetry. Narrow [S II] 6716, 6731 Å emission is seen along its red edge, presumably associated with the narrow Hα emission.

[O I].—SN 1979C's late-time [O I] 6300, 6364 Å emission profile is double-peaked much like that reported by FM93 but with different peak velocities. From the MMT spectrum, we measure peaks at 6230 and 6320 Å (-4900 and -600 km s^{-1} if attributed to just the 6300 Å line), whereas FM93 found peaks at 6214 and 6329 Å (-5700 and -190 km s^{-1}). However, [O I]'s full expansion velocity in the MMT spectrum is -6300 to -1300 km s^{-1} and in good agreement with FM93. A 1998 June 2.4 m MDM [O I] image of SN 1979C taken using the same filter used by FM93 indicates a 10% increase in [O I] luminosity between 1991.5 and 1998.5.

[O II].—FM93 identified the emission near 7300 Å as [O II] 7319, 7330 Å based upon the excellent match of the feature's double-peaked velocity profile with the [O I] emission peaks. Two strong emission peaks can also be seen in the MMT spectrum at 7240 and 7347 Å. These correspond to -5000 and -700 km s^{-1} in M100's rest frame, in agreement with the above measured [O I] peak velocities. This is graphically shown in Figure 4*b* and helps validate the [O II] identification made for the SN 1980K spectrum. We note that the [O II] 7319, 7330 Å emission appears stronger in 1993 relative to [O I] when compared with 1991/1992 data (FM93), making it now the strongest feature in SN 1979C's optical spectrum.

[O III].—The MMT spectrum of SN 1979C also shows broad, strong [O III] emission centered at 4965 Å and spanning 4880 to 5060 Å, which translate to -6300 to $+1600$ km s^{-1}. No emission peaks like those seen for [O I] and [O II] are evident from these data. We measure an observed [O III] flux of 3.5×10^{-15} ergs cm^{-2} s^{-1}.

Broad emission at 5750 Å.—Weak but very broad emission is also seen near 5750 Å and extending from 5550 to 6000 Å. Though faint, this emission is consistent with an earlier report of broad emission at 5700–5900 Å by FM93. Possible identifications include blends of [N II] 5755 Å, Na I 5890, 5896 Å, and He I 5876 Å.

3.2.2. *HST FOS Spectrum*

Figure 6 shows the combined 1997 FOS spectra (G270H and G400H) of SN 1979C covering the wavelength region 2200 to 4750 Å. The continuum levels at the G270H/G400H 3250 Å crossover point agreed quite well and no zero-point correction was applied.

Three prominent emission lines were detected below 3000 Å: C II] 2324, 2325 Å, [O II] 2470, 2470 Å, and Mg II 2796, 2803 Å. These lines show clumpy and strongly asymmetric profiles with the blueward peaks about twice as bright as those along the redward side, suggestive of internal dust extinction of the receding emission regions. Sharp blue emission peaks in these lines match well those seen in the optical lines from the MMT spectrum; specifically, the C II], [O II], and Mg II emission peaks at 2297 Å, 2440 Å, and 2767 Å correspond to the roughly -5000 km s^{-1} peaks in the [O I] 6300 Å and [O II] 7325 Å optical lines. The Mg II 2800 Å line appears broader than the two other UV lines, and this might indicate the presence of weak Mg I 2852 Å along its red wing. It is also possible that weak Si II] 2335 Å emission might also be blended with the C II] 2324, 2325 Å feature.

The [O II] 2470 Å lines arise from the same upper level

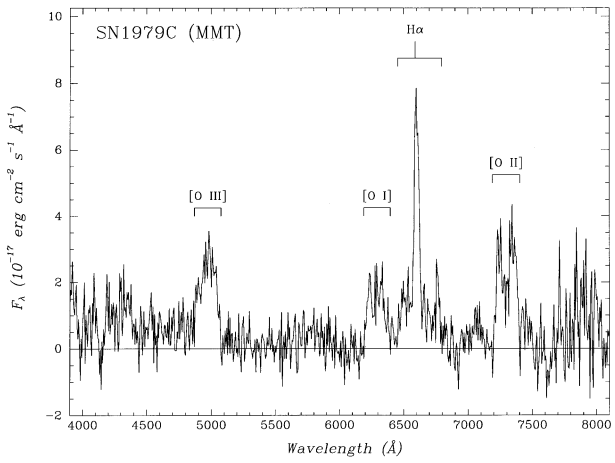

FIG. 5.—MMT spectrum of SN 1979C taken in 1993 May

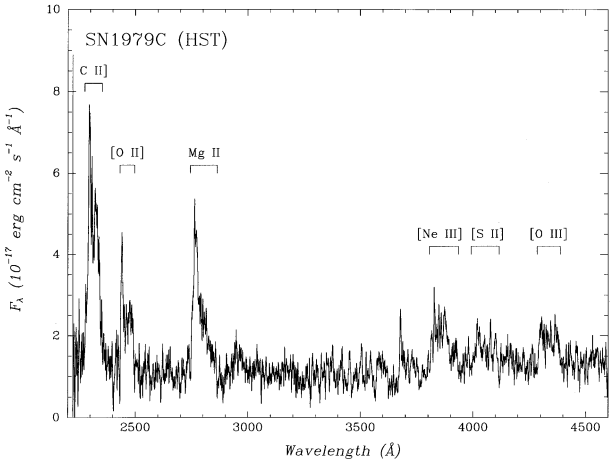

FIG. 6.—1997 FOS spectrum of SN 1979C

($2p^2\ ^2P$) as the near-IR [O II] 7319, 7330 Å lines. The relative strength of the $\lambda2470/\lambda7325$ ratio is determined by radiative transition probabilities (0.78; Mendoza 1983) and thus can be used to derive an estimate of the foreground extinction. Assuming no contribution from [Ca II] 7291, 7330 Å, the observed $\lambda2470/\lambda7325$ ratio of 0.21 ± 0.02 suggests that $E(B-V) = 0.27 \pm 0.2$ mag. However, this includes dust extinction within the SN's ejecta as indicated by the weaker red emission peaks in these UV lines compared with the near-IR lines. Therefore, measuring only the blue emission peaks in the [O II] 2470 and 7325 Å lines, we find a $\lambda2470/\lambda7325$ ratio of 0.25 ± 0.02, which implies $E(B-V) = 0.23 \pm 0.02$ assuming $R = A_V/E(B-V) = 3.1$. This should be a reasonable estimate of the foreground extinction (both Galactic and in M100) for SN 1979C. However, it is larger than the previous total reddening value of 0.18 ± 0.04 estimated toward SN 1979C (de Vaucouleurs et al. 1981) and may indicate that some weak [Ca II] 7291, 7330 Å emission contributes to the 7300 Å feature's strength. This would make the $\lambda2470/\lambda7325$ ratio appear smaller and hence the reddening larger. Alternatively, there might have been changes in [O II] line strengths during the four-year interval between when the optical (1993) and UV (1997) data were taken.

One can also estimate the internal dust extinction in the young, developing remnant by comparing the red emission spikes in the [O II] 2470 and 7325 Å lines. The observed $\lambda2470/\lambda7325$ ratio of 0.15 suggests $E(B-V) = 0.34 \pm 0.05$, implying an internal reddening of $E(B-V) = 0.11$–0.16 in addition to the foreground $E(B-V)$ of 0.18–0.23. Although the evidence for internal extinction is strong due to the consistently weaker red emission spikes in the UV line profiles, our measurement is not very accurate from this single measurement. Although the red emission peak is comparable or slightly stronger than the blue in the optical lines of [O I] 6300, 6364 Å and [O II] 7319, 7330 Å, much greater variation in blue/red peak strengths is seen for the UV lines in the *HST* data. For example, the red emission peak in the [O II] 2470 Å line is about 45% as strong as the blue emission peak, around 65% in the C II] 2324 Å line, and less than 35% for the Mg II 2800 Å line.

Emission features detected between 3000 and 4600 Å in the short G400H exposure are considerably weaker and consequently have less certain identifications but appear to be [Ne III] 3869 Å, [S II] 4068, 4076 Å, and [O III] 4363 Å. The strength of the temperature-sensitive [O III] 4363 Å line is surprisingly large relative to the [O III] 4959, 5007 Å lines and suggests electron densities greater than 10^6 cm^{-3}. The only other viable line identification for the 4335 Å emission is Hγ. This seems unlikely, however, due to the weakness of the Hα emission. Finally, our detection of [S II] 4068, 4076 Å is tentative but would be consistent with the SN 1980K spectrum.

4. DISCUSSION

To date, five papers have been published on the late-time optical spectrum of SN 1980K plus one each on SN 1970G, SN 1979C, and SN 1986E. None of these, however, presented spectra of sufficient S/N or covered a wide enough wavelength range to constrain several basic physical parameters such as densities or internal extinction, or test current late-time emission models. The new SN 1979C and SN 1980K spectra do provide some of this information and give a much clearer picture for late-time optical and UV properties of SNe II-L. In addition, because SN 1979C and SN 1980K were observed at comparable ages, they can be used to gauge the spread of SN II-L late-time emission properties.

4.1. *Late-Time Optical Properties of SNe II-L*

Table 1 lists the observed emission properties of four Type II-L SNe having detected late-time optical emission. They can be seen to exhibit several spectral similarities. From $\sim$8 yr and extending at least to 17 yr, the strongest optical emission lines in SNe II-L are Hα, [O I] 6300, 6364 Å, [O II] 7319, 7330 Å, and [O III] 4959, 5007 Å. These lines show similar expansion velocities, $\sim$5000–6000 km s^{-1}, often with roughly equal line strengths. Several of these lines also have emission profiles showing evidence for dust formation by virtue of diminished flux from the receding emission portions. The presence of this dust extinction creates both blueshifted line centers and asymmetric blue line profiles. In addition, all four SNe show narrow emission lines (e.g., Hα and [O III]), which could imply similar interstellar environments for the progenitors such as local H II regions.

However, significant spectral differences also exist. Hα luminosities cover more than an order of magnitude, with a factor of 6 difference between objects of similar age (e.g., 79C and 80K). SN 1970G and SN 1986E exhibit little, if any, broad [O III] emission, SN 1980K some, while in SN 1979C [O III] is stronger than Hα. Conversely, SN 1980K has fairly strong [Fe II] emission, both at 7155 Å and the blend at 5100–5300 Å, whereas SN 1979C and the other two do not. In addition, the very broad, unidentified emission near 5750 Å in SN 1979C is not seen in SN 1980K.

Bright optical emission appears correlated with the presence of strong late-time radio nonthermal emission and inferred high mass-loss rates (see Table 1) in the sense that Hα luminosity tracks fairly well the peak 6 cm radio luminosity and the derived mass-loss rate from late-time radio data. For example, SN 1979C is the brightest radio and optical SN and has the largest estimated mass-loss rate, while SN 1970G is optically the faintest with the lowest estimated mass-loss rate. However, this correlation is not a particularly tight one. SN 1986E is nearly as bright optically as SN 1979C, yet it is quite faint in the radio. Moreover, strong radio emission is also not always a predictor of bright optical emission. Two of us (R. A. F. and A. V. F.) have been unsuccessful in detecting late-time optical emission from SN 1968D in NGC 6946 (the same parent galaxy as SN 1980K) as a follow-up to its late-time radio emission recovery (Hyman et al. 1995). The lack of detectable optical emission may be related to SN 1968D's location closer to NGC 6946's center and in a dustier region (see Trewhella 1998 and Van Dyk et al. 1998a), which may be attenuating faint, late-time optical emission below the detection threshold.

Late-time, optical emission lines from SNe II-L appear surprisingly steady over time spans of many years. Our 1993 spectrum of SN 1979C indicated no decrease in Hα flux compared with 1990/1991 data (FM93) and actually showed a slight increase, as does a comparison of 1991 and 1998 [O I] images. Recent radio measurements indicate a flattening of its radio light curve (Van Dyk et al. 1998b) and new optical measurements should be undertaken. SN 1980K's Hα flux remained nearly constant from 1987

TABLE 1

OBSERVED AND PREDICTED LATE-TIME EMISSION FROM SNe II-L

Item	SN 1986E[a] NGC 4302	SN 1980K[b] NGC 6946	SN 1979C[c] NGC 4321	SN 1970G[d] NGC 5457	RSG Model[e]	Power-Law Model[e]	Power-Law Model[e]
Age at observation (yr)	8	14–15	12–14	22	10	10	17.5
Distance (Mpc)	16.8	7.5	17	7	...	...	...
$E(B-V)$ (mag)	0.02	0.40	0.23	0.15	...	...	...
Mass-loss rate[f]	4.7	2.0	19	2	...	...	...
Hα luminosity[g]	8.9	2.5	15	1	4.8	0.9	0.5
Peak radio luminosity[h]	1.1	1.0	26	1.5	...	...	...
Relative line fluxes[i]:							
Hα 6563	10, 10	10, 10	10, 10	10, 10	10	10	10
[O I] λλ6300, 6364	9, 9	7, 7	9, 9	6, 6	1	5	7
[O II] λλ2470, 2470	...	...	2, 6	...	...	...	...
[O II] λλ7319, 7330	3, 3	10, 9	12, 11	...	...	1	1
[O III] λ4363	...	1, 2	2, 3	...	...	...	...
[O III] λλ4959, 5007	<3, <5	2, 3	9, 11	<6, <7	34	23	46
C II λλ2324, 2325	...	...	6, 25	...	11	15	10
Mg II λλ2796, 2803	...	...	4, 9	...	49	79	57
[Ne III] λλ3868, 3869	...	...	2, 3	...	3	4	5
[S II] λλ4068, 4076	...	2, 4	1, 2	...	...	2	3
[Fe II] λ7155	<3, <3	3, 3	<5, <5	...	...	...	...
Detection upper limits:							
[O II] λλ3726, 3729	...	...	<1, <2	...	<1	2	5
Mg I] λ4571	...	<2, <4	<2, <4	...	3	6	4
[Na I] λλ5890, 5896	<3, <4	<2, <2	?	<5, <6	2	10	13
[N II] λλ6548, 6583	<3, <3	<5, <5	<5, <5	<5, <5	<1	5	7
[C I] λ8729	...	<2, <2	...	...	0	2	4
[S III] λλ9069, 9531	...	<3, <3	...	...	2	11	13
Expansion velocity (km s^{-1}):							
Hα λ6563 (blue)	−6000	−5700	−6300	−5400	...	...	...
Hα λ6563 (red)	+2600	+5500	+6300	+5300	...	...	...
[O I] λλ6300, 6364 (blue)	−7350	−6000	−6300	−6450	...	...	...
[O II] λλ7319, 7330 (blue)	...	−5000	−6300	...	...	...	...
[O II] λλ7319, 7330 (red)	...	+5000	+300	...	...	...	...
[S II] λλ4068, 4076 (blue)	...	−5500	...	...	...	...	...
[S II] λλ4068, 4076 (red)	...	+4000	...	...	...	...	...
Hα line asymmetry	Red?	Blue	Blue	Blue	...	...	...
Clumpy [O I] emission ?	Yes?	Yes	Yes	Yes	...	...	...
Narrow nebular lines ?	Yes	Yes	Yes	Yes	...	...	...

[a] Cappellaro et al. 1995. Note that we identify [O II] instead of [Ca II] as the line observed at 7300 Å in SN 1986E.
[b] This paper and Fesen et al. 1995.
[c] This paper and Fesen & Matonick 1993.
[d] Fesen 1993.
[e] Chevalier & Fransson 1994.
[f] In units of 10^{-5} yr^{-1} $M_{\odot}$; values are from Montes et al. 1997 and Weiler et al. 1993.
[g] In units of 10^{37} ergs s^{-1}; values calculated using $E(B-V)$ and distances quoted.
[h] Peak 6 cm luminosity in units of 10^{26} ergs s^{-1} Hz^{-1}; Montes et al. 1997, Weiler et al. 1993, and Cowan et al. 1991.
[i] Listed relative to Hα = 10. For entries with two values, the first, $F(\lambda)$, refers to the observed line fluxes, and the second, $I(\lambda)$, refers to fluxes corrected for reddening and narrow-line components.

through 1994, decreasing only recently. In Figure 7, we show the Hα light curve over one decade: from 1987 through 1997. The data indicate no change between 1987 and 1992.5. Spectra taken in 1991.4 and 1992.5, though indicating possibly a slow fading, were of lower quality than one obtained in 1992.6, which indicated no significant drop in Hα strength (FM94). Moreover, broadband photometric studies covering the years 1990–1992 indicated SN 1980K's optical flux level remained virtually unchanged from that seen in 1987, especially in the R band, which is sensitive to Hα emission ($R = 21.9 \pm 0.1$ mag; Leibundgut et al. 1993).

A more recent spectrum taken in 1994, however, showed an Hα emission flux of $(1.4 \pm 0.2) \times 10^{-15}$ ergs cm^{-2} s^{-1} (FHM95), about 25% less than the 1.7×10^{-15} ergs cm^{-2} s^{-1} found earlier. Our 1997 measurement of $(1.3 \pm 0.2) \times 10^{-15}$ ergs cm^{-2} s^{-1} supports a fading Hα strength, which may have started during the last several years, possibly in 1994 with the decline reported in FHM95. While this optical fading would roughly coincide with a drop in radio emission (Montes et al. 1998), we cannot completely rule out a small, steady decline in Hα over the 1987–1997 period from the spectroscopic data.

During $t = 10$–20 yr, SN 1980K's broad Hα line profile gradually narrowed, changing from a FWHM = 220 Å in 1988.6 to 190 Å in 1997.9 (see Fig. 3). This trend has been noted earlier (FM94) and is predicted by SN-CSM interaction models (CF94). However, Hα appears to be the line most affected, with the [O I] 6300, 6364 Å line profile changing little during this time interval.

With the notable exception of Hα, all the broad emission lines exhibit a spiky profile suggestive of clumpy emission regions at particular velocities. This is perhaps most clearly

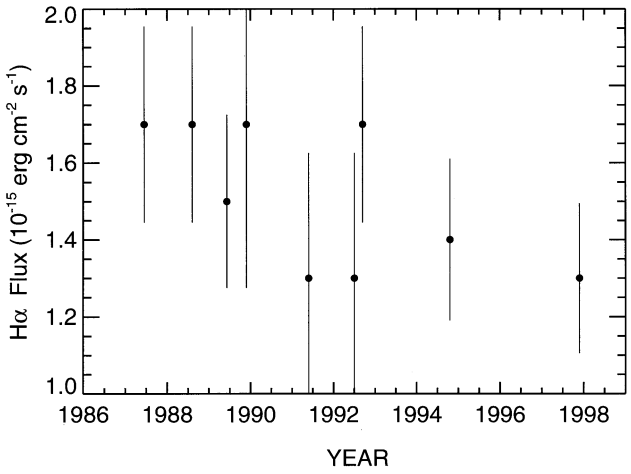

FIG. 7.—Plot of observed Hα flux measurements for SN 1980K taken since 1987.

seen in SN 1979C, where emission peaks at -5000 and -1000 km s^{-1} can be seen in the [O I] 6300 Å, [O II] 2470 Å, [O II] 7325 Å, C II] 2324 Å, and Mg II lines. The less blueshifted emission peaks are always weaker in the UV lines compared with the red or near-IR lines, consistent with the presence of internal extinction. In a similar fashion, SN 1980K also exhibits strong emission peaks in the [O I] 6300 and [O II] 7325 Å lines. The fact that the Hα profile in both SN 1979C and SN 1980K does not show such emission peaks suggests that the O-, C-, Mg-rich emitting material is coming mostly from ejecta and is physically separate from the dominant Hα emitting material, which includes the swept-up shell.

Our new spectra also allow one to get a handle on the electron density and temperature. In SN 1980K, we detected [S II] 4068, 4076 Å lines but not [S II] 6716, 6731 Å emission. The [S II] 4068, 4072 Å lines have a critical density, n_{cr}, of 1.3×10^6 cm^{-3}, whereas the 6731 Å line has $n_{cr} = 1.5 \times 10^4$ cm^{-3}. This suggests collision deexcitation of the [S II] 6716, 6731 Å lines due to electron densities near 10^5–10^6 cm^{-3}. An upper limit of $\sim 10^7$ cm^{-3} is suggested by the presence of strong [O I] 6300, 6364 Å emission ($n_{cr} = 1.6 \times 10^6$ cm^{-3}) and [O II] 7319, 7330 Å ($n_{cr} = 3 \times 10^6$ cm^{-3}), although [O I] 6300, 6364 Å emission can be strong even at high densities because it is an important coolant for low-ionization gas. For example, [O I] emission is important for the cool shell in the CF94 models even though $n \sim 2 \times 10^8$ cm^{-3}. If SN 1979C's densities were similar to those of SN 1980K, we would predict little [O II] 3726, 3729 Å emission, which has $n_{cr} = 5 \times 10^3$ cm^{-3}, and this agrees with observation. Indeed, the FOS spectrum of SN 1979C reveals strong [O II] 2470 Å emission but virtually no [O II] 3727 Å emission.

As shown in Table 2, only those emission lines with critical densities above 10^5 cm^{-3} are detected in both 79C and 80K. Consequently, we conclude that all lines with critical densities below 10^5 cm^{-3} are collisionally suppressed relative to lines having higher critical densities. Electron densities of (1–3) $\times 10^6$ cm^{-3} would also explain the observed low ratio of [O III] ($\lambda\lambda$4959 + 5007)/λ4363. The [O III] 4959, 5007 Å lines have $n_{cr} = 6.2 \times 10^5$ cm^{-3}. If the electron densities were a bit above 1×10^6 cm^{-3}, then the normally strong [O III] lines would be suppressed relative to [O III] 4363 Å line intensity ($n_{cr} = 2.6 \times 10^7$ cm^{-3}). Furthermore, the [O III] electron temperature must be greater than $\sim$15,000 K (i.e., $I(\lambda\lambda 4959 + 5007)/I(\lambda 4363) \simeq 4$ assuming $n = (2\text{–}5) \times 10^6$ cm^{-3}) in order to generate sufficient 4363 Å emission to be detected given the S/N of the data.

A very broad emission feature seen in SN 1979C's spectrum near 5800 Å may be partially due to the temperature-sensitive [N II] 5755 line. If correct, this would also indicate a [N II] temperature above 10^4 K. The overall weaker [O III] emission seen in the SN 1980K spectrum might be due to low ejecta ionization as indicated by the presence of strong [Fe II] 5050–5400 Å and 7155 Å emission.

4.2. *Observed versus Predicted Late-Time SNe II-L Emission*

Late-time optical observations of SNe II-L can be used to

TABLE 2

CRITICAL DENSITIES OF DETECTED AND NONDETECTED LINES

Density Range/Emission Lines	Critical Density[a] (cm^{-3})	Line Strength in SN 1980K (at 15 yr)	Line Strength in SN 1979C (at 14 yr)	Power-Law Model Predictions (at 17.5 yr)
$n_e \leq 10^5$ cm^{-3}:				
[N II] $\lambda\lambda$6548, 6583	8.0×10^4	Absent	Absent	Strong
[O II] $\lambda\lambda$3726, 3729	2.6×10^3, 4.8×10^3	Absent	Absent	Moderate
[S II] $\lambda\lambda$6716, 6731	1.6×10^3, 1.5×10^4	Absent	Absent	Weak
[Ne IV] $\lambda\lambda$2422, 2425	3.8×10^4, 1.4×10^5	...	Absent	Weak
$n_e = 10^5$–10^6 cm^{-3}:				
[O III] $\lambda\lambda$4959, 5007	6.2×10^5	Weak	Moderate	Very strong
[S III] $\lambda\lambda$9069, 9531	8.0×10^5	Absent?	...	Strong
$n_e \geq 10^6$ cm^{-3}:				
[O I] $\lambda\lambda$6300, 6364	1.6×10^6	Strong	Strong	Strong
[O II] $\lambda\lambda$2470, 2470	3.3×10^6, 5.7×10^6	...	Strong	...
[O II] $\lambda\lambda$7319, 7330	5.7×10^6	Strong	Strong	Weak
[O III] λ4363	2.6×10^7	Weak?	Weak	...
[S II] $\lambda\lambda$4069, 4076	1.3×10^6, 1.7×10^6	Weak	Weak	Moderate
[Ne III] $\lambda\lambda$3868, 3869	8.5×10^6	...	Moderate	Moderate
[Ne V] $\lambda\lambda$3346, 3426	1.4×10^7	...	Absent	Moderate
C II] $\lambda\lambda$2324, 2325	3.0×10^8, 7.2×10^9	...	Strong	Strong

[a] Evaluated for $T = 10^4$ K; values taken from IRAF/STSDAS task NEBULAR.IONIC by D. Shaw.

test emission predictions in CF94's recent SN-CSM models. In Table 1, we list CF94's predicted relative line intensities for $t = 10$ and 17.5 yr arising from SN-CSM interactions assuming either a power-law or red-supergiant (RSG) density gradient. There is a general agreement with the observed line list, although there are significant differences with the relative line intensities. The observed line widths are approximately those expected and the general picture of emission from circumstellar interaction is supported, but CF94 present two detailed models that appear not to be well matched to the conditions in SN 1980K and SN 1979C. The models are based on the explosion of a 20 $M_\odot$ red supergiant with two variations for the outer density profile. Although not ideal, these models do provide a starting point for discussing the current observations.

The RSG model predicts about the right Hα luminosity but weaker [O I] and stronger [O III] (relative to Hα) than observed in all four cases. On the other hand, the 10 and 17.5 yr old power-law models predict about the right Hα/[O I] ratio, but less [O II] 7319, 7330 Å emission, too much [O III] 4959, 5007 Å, and much weaker Hα luminosity than observed.

Larger discrepancies between observations and models are seen for several UV lines. Both RSG and power-law models predict Mg II 2800 Å to be the dominant UV/optical line (after Lyα) at a strength 5–8 times more than Hα. However, the SN 1979C spectrum shows Mg II to be slightly weaker than Hα, with the strongest line actually being C II] 2324, 2325 Å. Likewise, Mg I] 4571 Å is predicted to be about one-half the strength of Hα yet is not seen in either 79C or 80K. Large differences between observed and predicted Mg II intensities are a problem common in young, O-rich SNRs (Blair, Raymond, & Long 1994; Sutherland & Dopita 1995) and may simply be indicating an incorrect assumed Mg abundance. However, large differences exist for other UV lines, such as C II] 2324, 2325 Å, which is about twice the predicted strength, and this difference grows somewhat larger if internal SN dust extinction is considered.

Other notable differences involve the [O II] lines. We find strong [O II] 7319, 7330 Å emission in both SN 1979C and SN 1980K and suspect its presence in SN 1986E, where it may have been misidentified as [Ca II] 7291, 7330 Å (Cappellaro et al. 1995). But [O II] 7319, 7330 Å emission is weak in all CF94 models, due to the high excitation energy of the upper [O II] level and its small collision strength. Because of this CF94 argued that [Ca II] was the chief source of line emission observed near 7300 Å. However, in view of the new spectra, it now appears quite likely that the majority of the 7300 Å emission is due to [O II]. The presence of strong [O II] 2470 Å supports this conclusion. Since CF94 do not predict a 2470 Å line strength, we cannot make a direct comparison. But based upon the theoretical [O II] λ2470/λ7325 ratio of 0.78, the model prediction should be about an order of magnitude too low.

Although [O II] 7319, 7330 Å lines are weak in most photoionized nebulae, the presence of strong [O II] emission in young SNRs is not uncommon. In almost all young, O-rich SNRs such as Cas A (SN 1680), as well as in SN 1957D (Cappellaro, Danziger, & Turatto 1995) and SN 1986J (Leibundgut et al. 1991), one finds strong [O II] 7325 Å emission, which is equal to or stronger than the other forbidden oxygen line emissions. Strong [O II] emission has been successfully modeled by Sutherland & Dopita (1995) using a mixture of shock and photoionized emissions zones in O-rich ejecta.

Additional model observation differences include the Ca II IR triplet and the [S III] 9069, 9531 Å lines. These emission lines are predicted to be strong in the power-law models but are not detected in the published near-IR spectrum of SN 1980K (FHM95). Finally, the favored power-law models predict a steady decline of the Hα emission and a rapid increase of [O III] 4959, 5007 Å (CF94).

Many model-observation differences appear to be related to higher electron and gas densities than the CF94 models assume. As noted above, the presence of strong [O III] 4363 Å emission indicates densities of 10^6–10^7 cm^{-3}. High oxygen gas densities would also account for the lack of any [O III] λλ4959, 5007 line discrimination in the [O III] profile for SN 1979C. At densities above 10^6 cm^{-3}, several lines predicted to be observable in the models, like [O II] 3727 Å, [N II] 6548, 6583 Å, and [S II] 6716, 6731 Å, will be strongly deexcited (see Table 2).

The differences indicate that the CF94 stellar model is not the best one to model SN 1979C or SN 1980K. Their assumed circumstellar density may also be a factor. Models for the light curves of these supernovae suggest an H envelope mass of ~ 1 $M_\odot$ (Swartz, Wheeler, & Harkness 1991; Blinnikov & Bartunov 1993; Arnett 1996), much lower than the mass assumed in CF94. With the low envelope mass, processed core material may not be strongly decelerated and could be moving at ~ 5000 km s^{-1}. Some deceleration of the core material could lead to hydrodynamic instabilities and clumping of the gas, which is consistent with the spiky profiles seen in the spectral lines of O, C, and Mg. If the gas is H-depleted core material, strong differences can be expected with the models of CF94, who assumed cosmic abundances.

The models presented in CF94 also assumed a circumstellar density determined by a mass-loss rate $\dot{M} = 5 \times 10^{-5}$ $M_\odot$ yr^{-1} for a wind velocity of 10 km s^{-1}. However, the analysis of the radio turn-on by Lundqvist & Fransson (1988) leads to $\dot{M} = 1.2 \times 10^{-4}$ $M_\odot$ yr^{-1} for SN 1979C for the same wind velocity. There is new evidence for a high circumstellar density around SN 1979C. Immler, Pietsch, & Aschenbach (1998) have detected X-ray emission from the supernova with *ROSAT* and determined a 0.1–2.4 keV X-ray luminosity of 1.0×10^{39} ergs s^{-1}. The summed luminosity of the observed lines listed in Table 1 is 1.3×10^{39} ergs s^{-1}, and this figure is likely to be substantially increased when unobserved lines such as Lα are included (CF94). In the circumstellar interaction model, the optical and ultraviolet lines are excited by the X-ray radiation, so the implication is that the X-rays from the reverse shock wave are being absorbed by the cool circumstellar shell. This would explain the observed constancy of the line emission because the X-ray emission at the reverse shock should decline slowly if the reverse shock is a cooling shock (CF94). Application of equation (2.17) of CF94 shows that the circumstellar shell can still be optically thick at 1 keV at the time of the observations if the density power law for the supernova is $n \approx 12$, where $\rho \propto r^{-n}$, or if the circumstellar density is about twice that quoted above. In the CF94 power-law density model at an age of 10 years, the supernova H density just inside the reverse shock front is 4×10^4 cm^{-3}. For SN 1979C, the density may be several times higher, but it still falls short of the density implied by the [O III] line ratio. The implication is that the [O III] lines are

formed inside of the reverse shock, which is consistent with the lack of narrowing of the lines with time.

5. CONCLUSIONS

From Keck and MDM optical spectra of SN 1980K and optical MMT and UV *HST* spectra of SN 1979C, we find the following:

1. The optical spectrum of SN 1980K taken at 15 and 17 yr shows continued strong and broad 5500 km s^{-1} emission lines of Hα, [O I] 6300, 6364 Å, and [O II] 7319, 7330 Å, with weaker but similarly broad lines of [S II] 4068, 4072 Å, Hβ, [Fe II] 7155 Å, and a [Fe II] blend at 5050–5400 Å. The presence of [S II] 4068, 4072 Å but a lack of [S II] 6716, 6731 Å emission suggests collisional deexcitation of the [S II] 6716 and 6731 Å lines due to electron densities of 10^5–10^6 cm^{-3}. The 1997 MDM spectra indicates a Hα flux of $(1.3 \pm 0.2) \times 10^{-15}$ ergs cm^{-2} s^{-1}, suggesting a 25% drop from 1987–1992 levels sometime during the period 1994 to 1997, possibly simultaneously with an observed decrease in nonthermal radio emission.

2. Like SN 1980K, SN 1979C's optical spectrum at $t = 14.0$ yr shows $\sim$6000 km s^{-1} wide emission lines but weaker Hα, strong [O III] 4959, 5007 Å, clumpy [O I] and [O II] line profiles, no detectable [Fe II] 7155 Å emission, and a faint but very broad emission feature near 5750 Å. A 1997 *HST* Faint Object Spectrograph spectrum covering the range 2200–4500 Å shows strong lines of C II] 2324, 2325 Å, [O II] 2470 Å, and Mg II 2796, 2803 Å along with weaker [Ne III] 3969 Å, [S II] 4068, 4072 Å, and [O III] 4363 Å. A lack of [O II] 3726, 3729 Å emission, together with a [O III] $(\lambda\lambda 4959 + 5007)/\lambda 4363 \simeq 4$, indicates electron densities $\sim 10^6$–10^7 cm^{-3}. Furthermore, the [O III] temperature must be greater than $\sim$15,000 K in order to generate sufficient 4363 emission to be so easily detected [i.e., $I(\lambda\lambda 4959 + 5007)/I(\lambda 4363) \simeq 4$ assuming $n = (2$–$5) \times 10^6$ cm^{-3}]. A very broad emission feature seen in SN 1979C's spectrum near 5800 Å may be partially due to the [N II] line at 5755 Å.

3. In both SN 1979C and SN 1980K, several lines show one or more sharp emission peaks. The blueward peak(s) are substantially stronger than those toward the red, indicating internal dust extinction with the expanding ejecta. The amount of internal extinction in SN1979C is estimated to be $E(B - V) = 0.11$–0.16 mag. The line profile differences exhibited between Hα and the oxygen lines suggests that we are seeing emission from two or more separate regions, possibly the shell (Hα) and the inner SN ejecta (O lines).

4. Comparison of these observations to late-time SN model predictions indicates several areas of significant differences, many of which can be attributed to model electron densities being several orders of magnitude too low. For example, [O II] 3727 Å emission is predicted to be moderately strong in the models but is not seen due to densities well above the [O II] critical density of 4×10^3 cm^{-3}. In other cases, such as Mg II 2800 Å, which arises chiefly from the swept-up shell, the observed emission is far weaker than predicted. The parameters for future models will have to be more closely adapted to the conditions in these supernovae.

It should be noted that other SNe II besides Type II-L can exhibit bright, late-time optical emission, most notably the Type IIn objects SN 1986J (Leibundgut et al. 1991) and SN 1988Z (Filippenko 1991; Stathakis & Sadler 1991; Turatto et al. 1993). These objects show quite a different optical spectrum from the SNe II-L discussed above and are believed to be encountering dense, clumpy CSM (Chugai 1993; Chugai & Danziger 1994). The current, single Type II-P detection of SN 1923A in M83 in the radio (Eck, Cowan, & Branch 1997, Weiler et al. 1998) together with the lack of any reported late-time optical detections of SNe II-P suggests significant mass-loss differences between SNe II-L and II-P. It will be interesting to see whether SN 1923A can be recovered optically and how its UV and optical emission properties compare with those of SNe II-L.

Into what kind of young remnants will these SN II-L emission nebulae evolve? Except for the higher densities and the presence of strong hydrogen emission, the observed late-time spectra of SNe II-L bear some resemblance to Galactic and LMC O-rich SNRs such as Cas A and 1E 0102−7219 (Kirshner & Chevalier 1977; Blair et al. 1989). Their O, S, and C emission-line–dominated spectra with expansion velocities around 5000 km s^{-1} are not unlike those seen in 10^2–10^3 yr old O-rich SNRs. The weakness of [O III] 4959, 5007 emission and the absence of lines like [O II] 3727 Å, [Ne IV] 2425 Å, and [Ne V] 3426 Å can be attributed to higher filament densities and lower ionization levels.

However, it is not at all clear whether the progenitors of these older, metal-rich remnants are related to SNe II-L events. In the case of Cas A, the progenitor may have been a WN star, quite different from the RSG progenitor usually assumed for SNe II-L. Moreover, the Cas A supernova appears to have been subluminous and thus very different from the superluminous SN II-L events SN 1979C and SN 1980K. This all raises the issue of whether SNe of different types can yet leave similar-looking young remnants at ages 10–100 yr. If SN 1979C and SN 1980K remain luminous for several more decades, we may be able to address this question directly.

We are grateful to the staffs of the Keck, MMT, and MDM Observatories for their excellent observing assistance, and K. Weiler and M. Montes for generously communicating their radio study results on SN 1980K prior to publication. Financial support for this work was provided by NASA through grants GO-6043, GO-6584, and AR-6371 from the Space Telescope Science Institute, which is operated by the Association of Universities for Research in Astronomy, Inc., under NASA contract NAS 5-26555. We also acknowledge NSF grants AST 95-29232 to R. A. F. and AST 94-17213 to A.V. F.

REFERENCES

Arnett, W. D. 1996, Supernovae and Nucleosynthesis (Princeton: Princeton Univ. Press)
Barbon, R., Ciatti, F., & Rosino, L. 1979, A&A, 72, 287
Blair, W. P., Raymond, J. C., Danziger, J., & Matteucci, F. 1989, ApJ, 338, 812
Blair, W. P., Raymond, J. C., & Long, K. S. 1994, ApJ, 423, 334
Blinnikov, S. I., & Bartunov, O. S. 1993, A&A, 273, 106
Burstein, D., & Heiles, C. H. 1982, ApJS, 54, 33
Cappellaro, E., Danziger, I. J., & Turatto, M. 1995, MNRAS, 277, 106
Chevalier, R. A. 1982, ApJ, 259, 302
Chevalier, R. A., & Fransson, C. 1994, ApJ, 420, 268 (CF94)
Chugai, N. N. 1993, ApJ, 414, 401
Chugai, N. N., & Danziger, I. J. 1994, MNRAS, 268, 173
Cowan, J. J., Goss, W. M., & Sramek, R. A. 1991, ApJ, 379, L49
de Vaucouleurs, G., de Vaucouleurs, A. Buta, R., Ables, H. D., & Hewitt, A. V. 1981, PASP, 93, 36

Eck, C. R., Cowan, J. J., & Branch, D. 1997, BAAS, 191, 3901
Fesen, R. A. 1993, ApJ, 413, L109
———. 1998, AJ, 115, 1107
Fesen, R. A., & Becker, R. H. 1990, ApJ, 351, 437 (FB90)
Fesen, R. A., & Hurford, A. P. 1996, ApJS, 106, 563
Fesen, R. A., Hurford, A. P., & Matonick, D. M. 1995, AJ, 109, 2608 (FHM95)
Fesen, R. A., & Matonick, D. M. 1993, ApJ, 07, 1104 (FM93)
———. 1994, ApJ, 428, 157 (FM94)
Filippenko, A. V. 1991, in SN 1987A and Other Supernovae, ed. I. J. Danziger & K. Kjar (Garching: ESO), 343
Gaskell, C. M. 1992, ApJ, 389, L17
Hurst, G. M., & Taylor, M. D. 1986, J. British Astron. Assoc., 96, 102
Hyman, S. D., Van Dyk, S. D., Weiler, K. W., & Sramek, R. A. 1995, ApJ, 443, L77
Immler, S., Pietsch, W., & Aschenbach, B. 1998, A&A, 331, 601
Kirshner, R. P., & Chevalier, R. A. 1977, ApJ, 218, 142
Leibundgut, B., Kirshner, R. P., Pinto, P. A., Rupen, M. P., Smith, R. C., Gunn, J. E., & Schneider, D. P. 1991, ApJ, 372, 531
Leibundgut, B., Kirshner, R. P., & Porter, A. C. 1993, BAAS, 182, 2910
Lundqvist, P., & Fransson, C. 1988, A&A, 192, 221
Mendoza, C. 1983, in IAU Symp. 103, Planetary Nebulae, ed. D. R. Fowler (Dordrecht: Reidel), 143
Montes, M. J., Van Dyk, S. D., Weiler, K. W., Sramek, R. A., & Panagia, N. 1997, ApJ, 482, L61
———. 1998, preprint
Oke, J. B., & Gunn, J. E. 1983, ApJ, 266, 713
Oke, J. B., et al. 1995, PASP, 107, 375
Schmidt, G. D., Weymann, R. J., & Foltz, C. B. 1993, PASP, 101, 713
Stathakis, R. A., & Sadler, E. M. 1991, MNRAS, 250, 786
Sutherland, R. S., & Dopita, M. A. 1995, ApJ, 439, 381
Swartz, D. A., Wheeler, J. C., & Harkness, R. P. 1991, ApJ, 374, 266
Trewhella, M. 1998, MNRAS, 297, 807
Turatto, M., Cappellaro, E., Danziger, I. J., Benetti, S., Gouiffes, C., & Della Valle, M. 1993, MNRAS, 262, 128
Uomoto, A. 1991, AJ, 101, 1275
Uomoto, A., & Kirshner, R. P. 1986, ApJ, 308, 685
Van Dyk, S. D., Peng, C. Y., Barth, A. J., & Filippenko, A. V. 1998a, AJ, submitted
Van Dyk, S. D., Sramek, R. A., Weiler, K. W., Montes, M. J., & Panagia, N. 1998b, in ASP Conf. Ser. 144, Radio Emission from Galactic and Extra-Galactic Compact Sources, ed. J. A. Zensus, J. M. Wrobel, & G. B. Taylor (San Francisco: ASP), 357
Weiler, K. W., Panagia, N., Sramek, R. A., van der Hulst, J. M., Roberts, M. S., & Nguyen, L. 1989, ApJ, 336, 421
Weiler, K. W., Sramek, R. A., Panagia, N., van der Hulst, J. M., & Salvati, M. 1986, ApJ, 301, 790
Weiler, K. W., Van Dyk, S. D., Montes, M., Panagia, N., & Sramek, R. A. 1998, ApJ, 500, 51
Weiler, K. W., Van Dyk, S. D., Panagia, N., Sramek, R. A., & Discenna, J. L. 1991, ApJ, 380, 161
———. 1993, in ASP Conf. Ser. 104, Massive Stars: Their Lives in the Interstellar Medium, ed. J. P. Cassinelli & E. B. Churchwell (San Francisco: ASP), 436
Young, T. R., & Branch, D. 1989, ApJ, 342, L79